

Delay Tracking & Fringe Stopping for the GMRT Correlator

Jayaram N Chengalur

18/Oct/98

Abstract

This report gives an introduction to delay tracking and fringe stopping as implemented at the GMRT. The basic formulae are presented, followed by calculations of the expected range in which the total delay, as well as the fringe rate are expected to lie. The calculations are based on the currently available co-ordinates of the antennas (i.e. GPS co-ordinates or astronomically derived co-ordinates) and the OTDR measurements of the fiber optic path length to the arm antennas.

It is found that there are hour angle and declination ranges for which baselines to the extreme arm antennas have differential delays which are more than what can be corrected in the Mk-IV correlator. This is independent of the delay bias chosen. However, by properly choosing the delay bias, it should be possible to ensure that at any one time only one extreme arm antenna is lost.

This delay correction problem is present only for the 16 MHz total bandwidth mode of the correlator. Possible solutions include introducing an additional (non adjustable) delay in the paths of the inner antennas.

1 Introduction

The quantity that an interferometer attempts to measure is the spatial coherence function of the incident electric field. This electric field itself is caused by radiation from some distant cosmic source. It can be shown that if

the spatial correlation function is measured on an infinite 2D plane then the brightness distribution of the source can be obtained via a fourier transform¹.

In an interferometer the incident electric field is converted into an electrical voltage in the antenna, and this signal after amplification is transported from the antenna to the correlator. The signals that arrive at the correlator from different antennas hence have different propagation and instrumental delays which have to be corrected for. After this delay correction, the correlation coefficient of the voltage signals from different antennas is identical to the required spatial correlation function of the incident electric field (apart from a constant scaling factor which can be obtained via astronomical calibration).

The GMRT correlator thus has three major functions (i) To correct for the various instrumental and propagation delays that occur in each signal path (Dly-DPC) (ii) to do a Fast Fourier Transformer on each input signal, (to give better frequency resolution) (FFT) and (iii) to multiply (channel by channel) these various input signals and accumulate the products (MAC). In this note we examine in detail the exact delay corrections that need to be applied for the specific case of the GMRT. General discussions on the need for delay compensation in interferometers can be found in the standard textbooks referred to above.

2 GMRT Specific Details

Figure 1 is a block diagram of the principal delays encountered in the signal path from any given GMRT antenna. There is a geometric delay τ_g (which occurs at the radio frequency ν_{RF} , and arises due to the path length differences between the source to the different antennas), then a delay in the SAW filter at the first IF (τ_{s_1} at ν_{IF_1}), then a delay in the SAW filter at the second IF (τ_{s_2} at ν_{IF_2}) and a transmission delay in the optical fiber at the same second IF (τ_{Fb} at ν_{IF_2}). In the CEB the signal is assumed to undergo no further delays until digitization. After digitization various delays and corrections are applied.

In the GMRT correlator, the delay correction is broken up into many parts (i) τ_I , the integral delay correction. This is an integer multiple of the sampling time. (ii) Φ_{NCO} which is a fringe rate (i.e. a time varying phase)

¹see eg. 'Interferometry & Aperture Synthesis in Radio Astronomy', by Thompson, Moran & Swenson, or 'Synthesis Imaging in Radio Astronomy', Perley et. al. eds

GMRT Delay Block Diagram

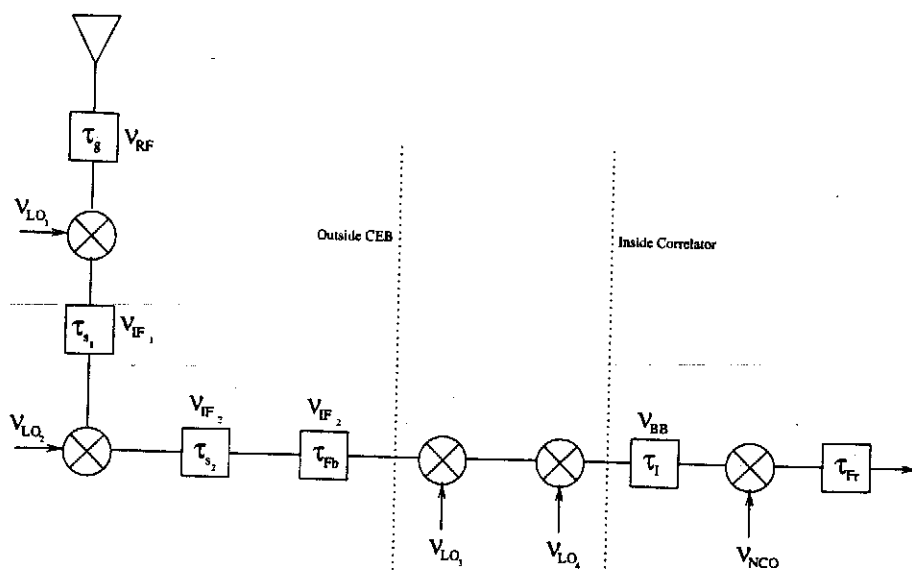


Figure 1:

that is applied to input sampled data by multiplying it with the output of a Number Controlled Oscillator (NCO), and (iii) τ_{Fr} , the Fractional Sampling Time Correction (FSTC) which is applied as a phase ramp across the band and could have a value that is not an integral multiple of the sampling time. Note that the first two corrections are applied in the time domain (i.e. before the FFT) while the last correction is applied in the frequency domain (i.e. after the FFT). In addition to these hardware corrections, any remaining residual correction (which arises, for eg. because of finite precision corrections in the correlator) could be applied by the DAS software. These corrections are discussed in more detail below.

All delays are measured with respect to some fixed (but as of yet unspecified) reference point. Just before entry into the MAC, the phase of the signal in frequency channel i (with frequency offset ν_i from ν_{BB}) from some given antenna compared to the phase of the signal at the reference point (which is assumed to go through the same LO chain, but with no associated delays apart from some reference delay τ_r at the baseband) is:

$$\Phi_i = 2\pi(\nu_{RF} + \nu_i)\tau_g + 2\pi(\nu_{IF_1} + \nu_i)\tau_{s_1} + 2\pi(\nu_{IF_2} + \nu_i)(\tau_{s_2} + \tau_{Fb}) - 2\pi(\nu_{BB} + \nu_i)(\tau_I + \tau_{Fr}) - \Phi_{NCO} - 2\pi(\nu_{BB} + \nu_i)\tau_r \quad (1)$$

It is assumed that USB mixers have been used throughout. This mixing scheme is the case of interest since it has the largest magnitude corrections. In practice the DAS software has to properly deal with USB and LSB separately. Before computing the cross-correlation we require to correct for all the propagation delays, i.e. we must ideally have $\Phi_i = 0$. In practice it is sufficient to have $\Phi_i = \text{constant}$, since this constant can be determined offline.

From equation (1) and the fact that $\nu_{BB}=0$, we have:

$$\frac{\Phi_i}{2\pi} = [\nu_{RF}\tau_g + \nu_{IF_1}\tau_{s_1} + \nu_{IF_2}(\tau_{s_2} + \tau_{Fb}) - \Phi_{NCO}] + \nu_i[\tau_g + \tau_{s_1} + \tau_{s_2} + \tau_{Fb} - \tau_I - \tau_{Fr} - \tau_r] \quad (2)$$

Where the corrections have been broken into a 'fringe' part (the first term) and a 'delay' part (the second term). An error in correcting the 'fringe' part will cause a phase error which does not depend on channel number, while an error in correcting the 'delay' part will cause a phase error that does depend on channel number. In the fringe part, all the terms except that associated with τ_g do not vary with time. Hence these terms can be ignored while computing Φ_{NCO} . (Ignoring these terms simply leads to an antenna based phase error, which will add to the phase errors introduced by the ionosphere and be removed in astronomical calibration). The 'delay' correction is done as follows. The integral part, as mentioned earlier is corrected using a variable length digital delay (τ_I), which in the GMRT case is implemented using a dual port RAM. This allows a correction in integer multiples of the sampling interval. The residual error which is less than one sampling interval will lead, as can be seen from eqn (2) to a phase error which increases linearly with increasing channel number. This phase ramp can be corrected by multiplying the output of the FFT with a signal with unity amplitude and with a phase ramp of the same magnitude as that caused by the delay correction error but with opposite sign. This is the 'fractional sampling time correction' or FSTC. While from eqn (2) it would appear that the total delay correction can be arbitrarily divided between τ_I and τ_{Fr} , it is important to keep τ_{Fr} as small as possible because otherwise the signal will be delayed beyond its coherence time and the correlation amplitude itself will start decreasing.

3 Numeric Values

For the GMRT antennas, (as we shall see below) τ_{Fb} and τ_g can both be several 10s of μsec . τ_{s_1} & τ_{s_2} , on the other hand are $\sim 2\mu\text{sec}$, and further since these filters occur in the signal path of all antennas and we are interested only in relative delays, it is only the unit to unit variations ($\Delta\tau_{s_1}$, $\Delta\tau_{s_2}$) in the SAW filters which enter into this equation. These unit to unit variations are very small (~ 2 nano-seconds), and can be ignored. The NCO which applies the fringe correction is tunable in steps of of 0.029/512 Hz. For the FSTC there are 32 lookup tables in which phase ramps can be stored. If one assumes that the FSTC is limited to ± 1 sampling interval, then one needs phase gradients going from 0 to ± 180 degrees across the entire band (i.e. 0 to ± 1.4 degrees/channel). The FSTC is hence accurate to 1/16 of the sampling interval. Additional inaccuracies will also be present because of finite precision mathematics in the correlator hardware. The maximum rate of change of geometric delay is $\sim \pm 3$ nano-seconds/second, and the maximum fringe rate (at 1450 MHz) is $\sim \pm 5$ Hz. These maximum rates are obtained for W06 and E06 for a source crossing the zenith.

Maximum Geometric Delays WRT C02

Ant	τ_{tot}^{max} μsec	τ_{geom}^{max} μsec	τ_{fix} μsec	h^{max} deg	δ^{max} deg
E02	27.7	2.7	18.4	-78.0	30.0
E03	50.4	5.6	34.7	-78.0	30.0
E04	78.3	8.3	52.2	-78.0	30.0
E05	108.6	9.3	74.9	-75.0	18.0
E06	131.6	13.0	90.9	-78.0	30.0
S01	33.3	-9.4	23.8	-12.0	-51.0
S02	50.9	-14.2	36.7	12.0	-51.0
S03	73.4	-21.4	52.2	-9.0	-51.0
S04	98.9	-30.0	68.9	-12.0	-51.0
S06	143.7	-44.4	99.3	6.0	-51.0
W01	14.5	2.2	9.1	78.0	30.0
W02	31.2	5.3	20.4	78.0	30.0
W03	56.3	10.5	37.4	78.0	30.0
W04	83.8	18.1	56.0	81.0	42.0
W05	113.7	27.4	77.4	81.0	45.0
W06	150.2	31.6	104.0	81.0	42.0

4 Limitations of the Mk-IV Delay Tracking

The correlator hardware (i.e. the RAM depth in the Dly-DPC card) allows for a tunable delay of upto 128 μsec . Simulations for the maximum delay expected were made using the OTDR measurements for the arm antennas as estimates of the fixed delay. For the central square antennas the geometric ('as the crow flies') distance was used to estimate the fixed delay, the expected corrections to the real life situation are small.

As can be seen from figure 2 there is a non trivial (h, δ) range for which

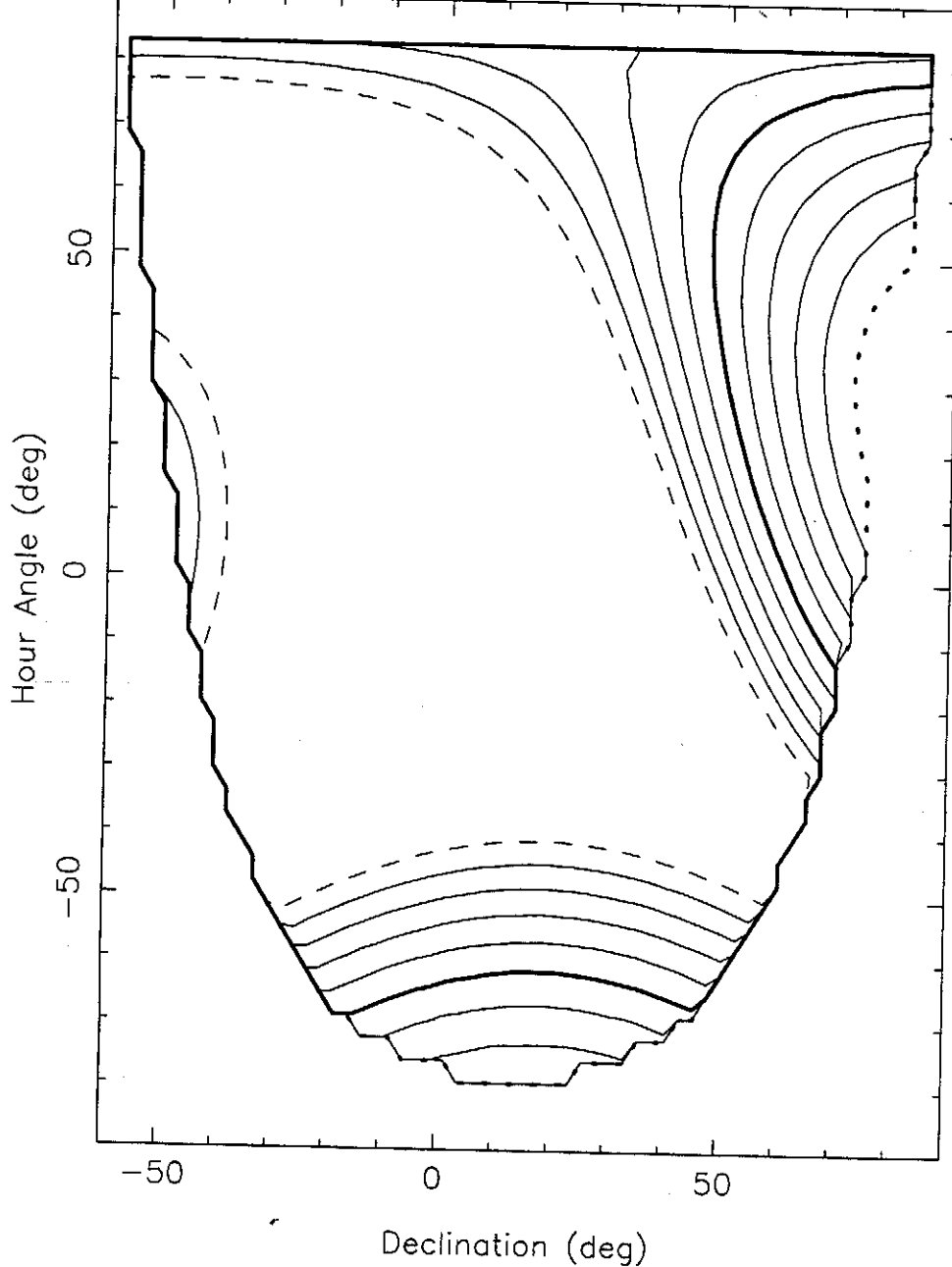
the simulated delay difference between the two antennas making up a given baseline is greater than $128 \mu\text{sec}$. These baselines are thus fundamentally lost, i.e. no adjustment of the delay bias can correct for the delay of both antennas in the baseline. The maximum delay difference that is obtained is $\sim 150 \mu\text{sec}$ between W06 and the central square for rising sources.

Figure 3[B] shows that at extreme declinations and hour angles, upto 2 antennas can have uncorrectable delays, if the delay bias is set to 2047. For a slightly smaller delay bias (1900) at most one antenna is lost at any given time. The exact antennas which are lost are given in Figure 3[A] for the case of a delay bias of 2047. Since there might be slight differences between the numbers used in this simulation and the real life situation, some fine tuning of the delay bias will probably have to be done using real observations.

For the 8 MHz total bandwidth, the total correctable delay becomes $256 \mu\text{sec}$, since the sampling interval is twice that at 16 MHz total bandwidth. This means that at 8 MHz and lower bandwidths the RAM depth is sufficient to allow delay correction for all sources that the antennas can be pointed at.

The problem arises primarily because of the long fiber delay suffered by the signals from the distant arm antennas. The fiber delay is of the order $105 \mu\text{sec}$ between W06 and the central square antennas. This means² that a possible solution is to add more digital delay to the central square antennas. Simulations show that if a fixed delay with value between $24 \mu\text{sec}$ and $115 \mu\text{sec}$ is added to all antennas in the central square *as well as* W01, W02, E02 and S01, then a further tunable delay of $128 \mu\text{sec}$ will allow delay correction for all observable sources even at 16 MHz total bandwidth.

²as suggested by the correlator group in note 'Preliminary Design Specifications for the New Dly-DPC System for GMRT Correlator' dated 21Sep98



units= μs scale fac = 1.0e+02 levs =
 1.28 1.30 1.32 1.34 1.36 1.38
 1.40 1.42 1.44 1.46 1.48

Figure 2: Contours show regions where the delay difference between two GMRT antennas exceeds $128 \mu\text{sec}$. The dashed contours are for $128 \mu\text{sec}$ delay, the heavy contour for $138 \mu\text{sec}$, and the dotted contour for $150 \mu\text{sec}$ delay. Where there is more than one baseline for which the delay difference between the two arms is greater than $128 \mu\text{sec}$, the contour indicates the baseline with the maximum delay difference.

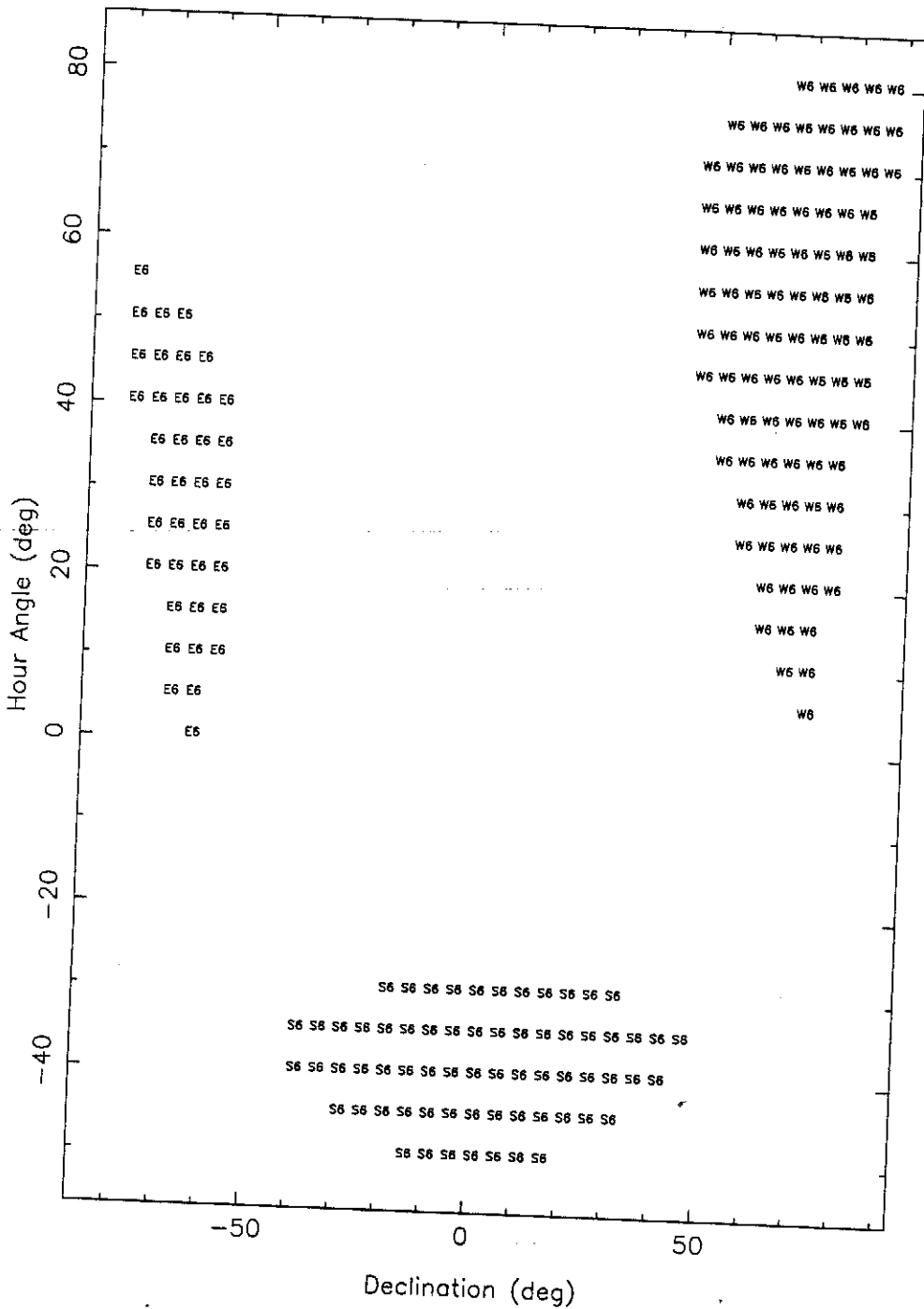


Figure 3: Hour angle and declination range for which the indicated antennas have a delay correction that exceeds the maximum settable correction in the Mk-IV Delay-DPC card, The delay bias has been chosen to be 2047 times the sampling interval.

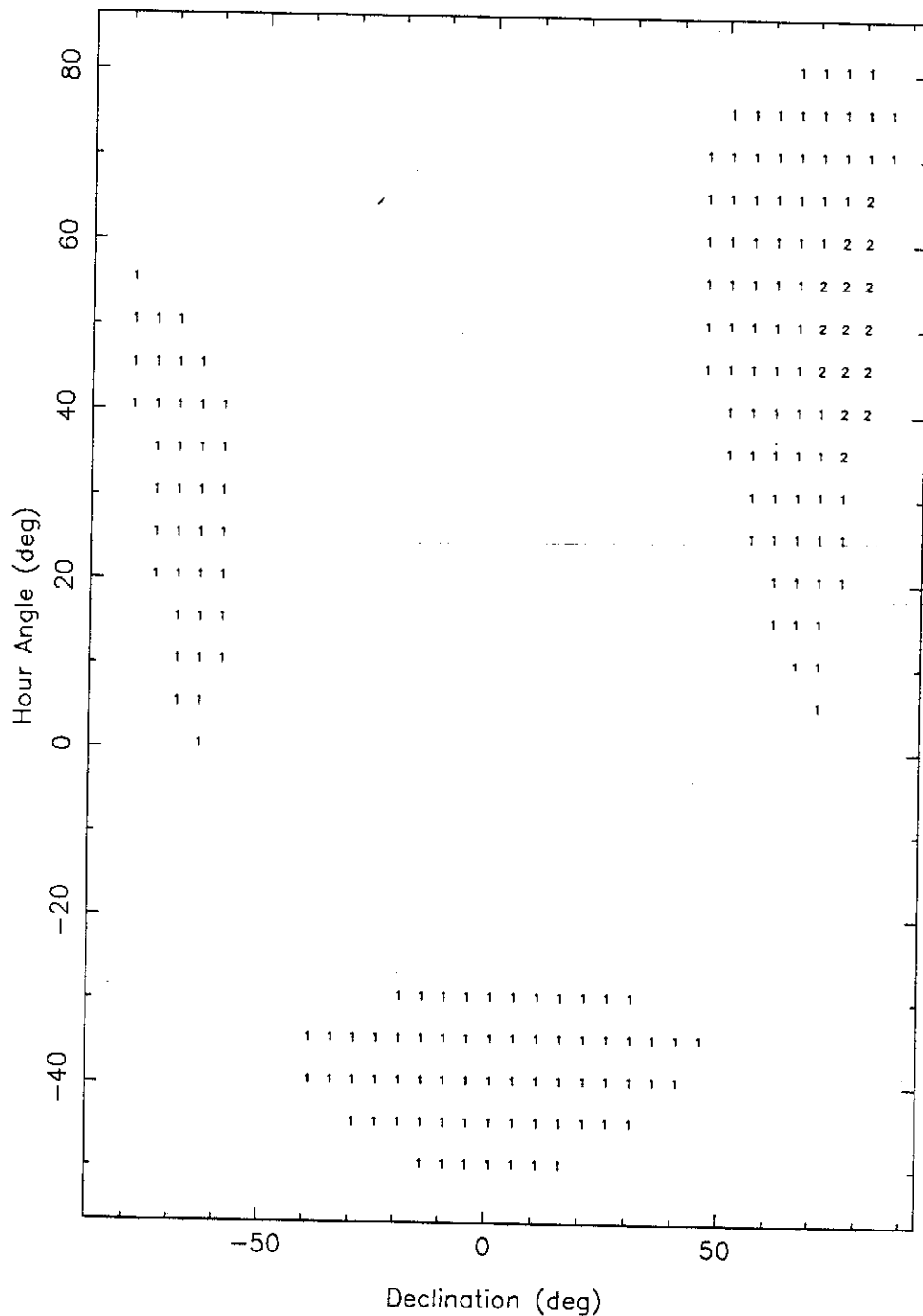


Figure 4: Total number of antennas that have a delay correction that exceeds the maximum settable correction in the Mk-IV Delay-DPC card as a function of hour angle and declination. The delay bias has been chosen to be 2047 times the sampling interval.